ARPN Journal of Engineering and Applied Sciences

EVALUATING SOIL SETUP AFTER OPEN METALLIC PILE DRIVING

Jamila El Brahmi, Othmane Hniad and Imane El Kasimi
Laboratoire d'Ingénierie Civile, Hydraulique et Environment (LINCHE), Mohammadia School of Engineers (EMI),
Mohammed V University in Rabat (UM5), RABAT, Morocco
E-Mail: elbrahmi@emi.ac.ma

ABSTRACT

After driving a pile, foundation soil is restructured and thus regains part of its resistance. This phenomenon is aptly named soil setup. This paper's focus is to study said phenomenon on eight open metal piles driven in a soil composed of sand and marl, while basing our findings on data of dynamic PDA tests processed with CAPWAP software. Firstly, dynamic tests performed after driving phase and at subsequent re-driving phases show an increase in both the required number of blows for a 10-centimeter drive and in the static resistance to re-driving. The correlations of these resistances with the predictions of the models of Skov & Denver (1988) and Svinkin & Skov (2000) were not satisfactory (R^2 of 0.77 and 0.75 respectively). Noting that the setup is mainly due to the increase in friction, a layer-by-layer analysis is carried out by treating the sand and the marl separately. Attained results fit well the Skov & Denver model and align with the experimental results of Murad (2014), but given the model's limitations in terms of reference time determination, we develop a new function model potency considering immediate setup. The new model fits our attained results very well (R^2 of 0.944 for sand and 0.980 for marl). The final static strength after setup is thus calculated as a function of time based on the power function model and conservative estimates. This approach encourages allowing time for the soil to gradually and naturally scar instead of rushing into immediate and costly measures such as patching.

Keywords: soil setup, open steel piles, re-driving resistance, PDA, CAPWAP.

Manuscript Received 10 September 2023; Revised 10 January 2024; Published 30 January 2024

INTRODUCTION

When driving a pile, the soil surrounding the pile's perimeter moves along its shaft radially and under its tip downwards. The soil is thus restructured and excess pore pressure is generated. After the driving process, excess pore pressure begins to dissipate by water flow, inducing shear resistance increase, and the soil is reconstituted and thus regains part of its resistance; this is what is called soil setup. This phenomenon takes place in three phases as is shown in Figure-1.

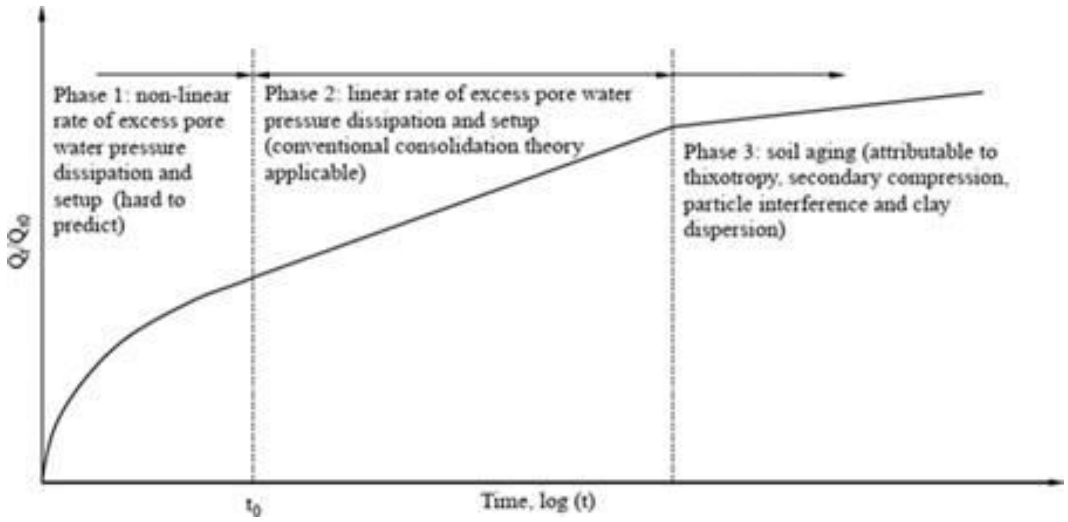

Figure-1. Idealized schematic of three main phases of pile setup (Source: Komurka et al. 2003).

- **Phase 1:** at the end of the driving phase, the soil is strongly disturbed and dissipation of excess pore pressure does not obey a linear curve with respect to logarithmic time. However, effective horizontal stress increases, the soil consolidates and its resistance also shows an increase.
- **Phase 2:** after a time period of t_0 (Figure-1), dissipation rate of the excess pore pressure becomes constant (linear) with respect to logarithmic time. The soil continues to consolidate; the horizontal stresses and the shear resistances also continue their increase.
- **Phase 3:** setup continues with an increasing shear modulus, stiffness and soil expansion while reducing its compressibility, independently of the effective stress which stabilizes. This is named the aging phenomenon (Schmertmann, 1991).

ARPN Journal of Engineering and Applied Sciences

To estimate this setup, there are empirical models which make estimating pile bearing capacity possible as the healing process progresses. The model of Skov & Denver (1988) suggests a semi-logarithmic empirical relationship describing setup in the following equation noted equation 1:

$$\frac{R_t}{R_0} = 1 + A \log(\frac{t}{t_0}) \quad (1)$$

Where:

- **R_t:** pile bearing capacity at a given time t after driving phase
- **R_0:** initial pile bearing capacity (at the end of driving phase)
- **A:** setup parameter
- **t_0:** benchmark time, start of setup phase 2 (Figure-1)

It should be noted that t_0 depends on the soil type and pile size. Skov and Denver recommend a 12-hour benchmark time for loose soils as opposed to 24 hours for cohesive ones. On the other hand, Svinkin (1994) used a t_0 of one to two days, and Bullock (1999) and Bullock & McVay (2005) recommended normalizing t_0 to equal one day. As for the setup parameter A, it depends on the soil and pile characteristics, but is not influenced by the depth or the dissipation of excess pore pressure (Camp & Parmar (1999), Svinkin (1994) and Skov & Svinkin (2000)). Moreover, and following the comparison of 14 researchers' results, Chow (1998) finds that A varies from 0.12 to 0.75. In addition, a setup study conducted at five different sites in Louisiana, USA rendered values of A averaging 0.2 and 0.67 for loose soils and cohesive soils respectively (Murad, 2014).

Svinkin and Skov (2000) presented another formula for setup estimation which takes into account elapsed time immediately after pile driving ends, which showed that benchmark time t_0 had no effect on the setup process. Said formula will be named equation 2:

$$R_t/R_{FB} - 1 = B (\log10 (t) + 1) \quad (2)$$

Where B is the setup factor.

STUDY DATA

The soil setup phenomenon is studied on the open metallic piles of a Moroccan port's container terminal. The terminal's quay is divided into seven zones according to the geotechnical profiles' homogeneity. The piles that will be studied to assess setup are located between zones 4 and 5 from PM-650 to PM-1100 which are shown in Figure-2.

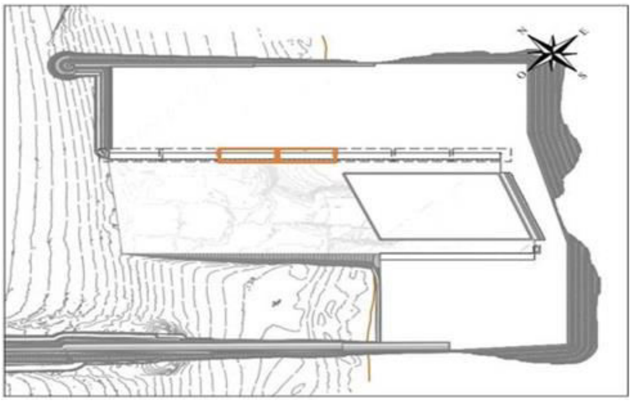

Figure-2. Study area localization in the project's general blueprint.

Eight open metal piles spread over three lanes (EA, EC and EE) were tested. Their locations are shown in Figure-3.

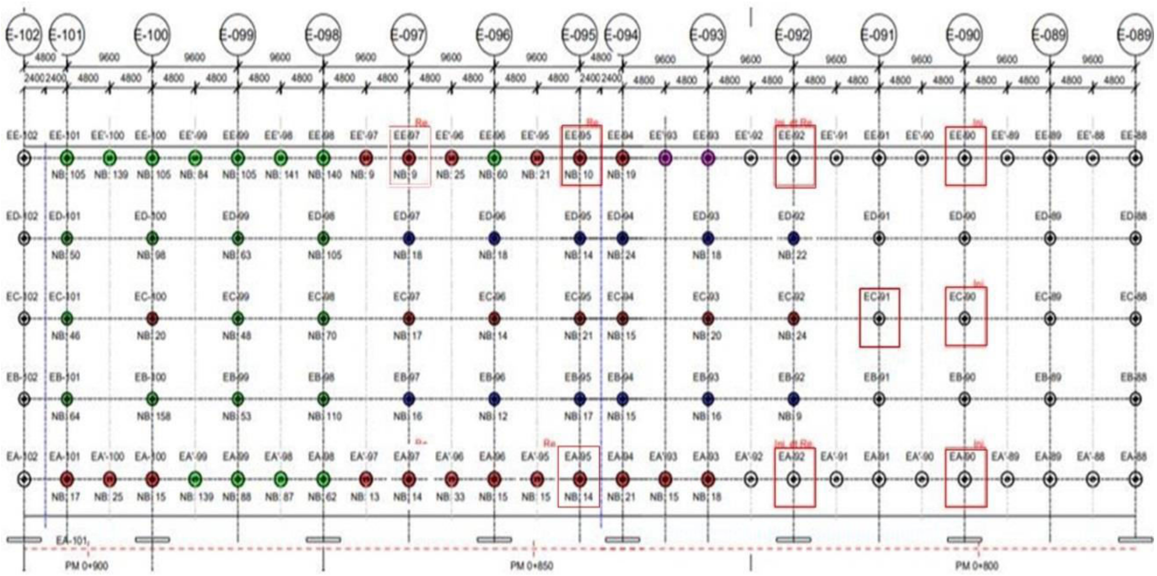

Figure-3. Plain view of the study area.

ARPN Journal of Engineering and Applied Sciences

Based on the geotechnical campaign (including drilling with laboratory tests, pressure meter tests and CPT tests), three geotechnical units were defined for the study area as detailed in Table-1. The piles studied are thus driven into a soil mainly composed of sand and marl.

Table-1. Definition and soil nature of the project's geotechnical units.

Geotechnical unit	Soil nature	Description
GU3	Dense to very dense sands	Sands from clean to loamy which turn into gravelly sands of depths reaching 9 meters
GU4	Green marl	A 2-meter-deep layer
GU5	Grey marl	Found along the ECT profiles reaching -80m ZH

The characteristics of the test piles are presented in Table-2.

Table-2. Study piles' characteristics.

Pile index	Diameter (mm)	Width (mm)	Length (m)	Soil stratification (depth in meters)				
				Embankment	Dense sands	Gravelly sands	Green marl	Grey marl
EE90	1422	20.6	38.59	12.33	4.58	1.00	2	17.5
EC90	1219	20.6	38.34	5.97	7.59	1.00	2	17.5
EA90	1422	20.6	38.41	1.00	-	0.90	2	17.5
EC91	1219	20.6	38.35	4.90	2.59	1.00	2	17.5
EA92	1422	20.6	40.37	1.00	-	0.93	2	17.5
EE95	1422	20.6	44.00	13.75	3.87	1.00	2	17.5
EE92	1422	20.6	39.34	12.33	5.13	1.00	2	17.5
EA95	1422	20.6	44	1	-	0.93	2	17.5

METHODOLOGY

The study of the setup phenomenon requires carrying out at least two pile loading tests, one at the end of the driving phase (FB) determining the initial resistance, and the other at the redriving phase (RB) conducted later, making it possible to measure strength gains and determine the setup progress over time.

Two types of tests can be used: the PDA dynamic load test and the static load test. The static load test is impractical for end-of-driving-phase measurements given the waiting time (of several days) required between pile placement test start, unlike the PDA which makes it possible to measure the pile responses during the driving phase, and thus the pile's resistance at the end of driving phase (FB). In this study, the results of the PDA test processed with the CAPWAP software are used.

We begin this study, initially, by analyzing the evolution of the number of blows required to drive the 10-centimeter test piles during the first series of re-driving (DR), compared to the one required to reach the same depth at the end of driving phase (FB). The number of blows per 10-centimeter drive for a uniform energy of 250KJ, is obtained by the following formula:

$$\text{blows/10cm} = N.\ \left(\frac{10}{E}\right)\left(\frac{En}{250}\right) \qquad (3)$$

Where:

- N: number of blows for a specific threshing ram energy
- E: driven length of the pile in centimeters
- En: Energy with which the pile is driven for a length equal to E

A global analysis based on the calculation of the setup rate and the ratio of re-driving resistance to end-of-driving-phase resistance (R_t/R_{FB}) was carried out for each of the piles, followed by an estimate of the setup progress by the Skov & Denver and Svinkin & Skov models. The prediction curves of the two models are compared to the actual test results that were presented in the overall analysis. The quality of the adjustment is assessed via the R^2 coefficient. A benchmark time of one day will be adopted for this analysis since the soil of the study area is mixed (sand and marl).

If the obtained correlation is not satisfactory, the study continues by dissociating the (measured) overall resistance due to setup into frictional and tip resistance, to determine each of the two resistances' contribution to

ARPN Journal of Engineering and Applied Sciences

improving overall resistance. A more in-depth study will be based on the main component of setup (which will most likely be friction according to Chow, 1998).

In this case, the two layers of soil surrounding the piles (sand and marl) will be treated separately, since said soils are very different, particularly with regard to grain size, structure and mechanical behavior. This layer-by-layer analysis will make it possible to develop a new model that takes into account the healing potential of each of the two layers and will make it possible to better predict the final resistance after setup.

To assess the final strength after the setup process, an approximate equation is established using the initial static strength of the pile before setup as a benchmark. Conservative estimates are used to determine a conservative setup rate that takes into account elapsed time and soil layers' characteristics which the pile traverses.

The bearing capacity of the pile before healing can be calculated by the following formula, named equation 4:

$$R_{\text{initial}} = q_S.S_S + q_m.S_m + q_{\text{tip}}S_p \quad (4)$$

Where:

- $\mathbf{q_S}$: friction resistance of the sand layer
- $\mathbf{S_S}$: area of the pile's lateral portion embedded in the sand
- $\mathbf{q_m}$: friction resistance of the marl layer
- $\mathbf{S_m}$: area of the pile's lateral portion embedded in the marl
- $\mathbf{q_{tip}}$: pile tip resistance
- $\mathbf{S_p}$: lateral section area of the pile's tip

Considering the three EE90, EE92 and EE95 piles of row E and L_S being the conservative factor between the three piles:

L_S=min (q_{S1} /q_{m1}, q_{S2} /q_{m2}, q_{S3} /q_{m3})
L_p=min (q_{p1} /q_{m1}, q_{p2} /q_{m2}, q_{p3} /q_{m3})

Which gives?

$$R_{\text{initial}} = L_s.q_m.S_S + q_m.S_m + L_p.q_mS_p$$

An, in turn, a final formula for the pile's initial bearing capacity expressed in equation 5:

$$R_{\text{initial}} = (L_s.\frac{S_S}{S_m} + 1 + L_p.\frac{S_p}{S_m}).q_mS_m \quad (5)$$

The pile's bearing capacity post-setup is shown in the following formula, named equation 6:

$$R_{\text{finale}} = K_S.q_S.S_S + K_mq_mS_m + q_{\text{pointe}}S_p \quad (6)$$

where K_S and K_M are the setup rates of sand and marl respectively, determined by the model adopted by the layer-by-layer analysis.

Expressing R_{final} using q_m and S_m, the following formula is obtained:

$$R_{\text{final}} = (L_s.\frac{S_S}{S_m}.K_S + K_m + L_p.\frac{S_p}{S_m}).q_mS_m$$

And, the K_t factor being time-dependent is as shown in equation 7:

$$K_t = \frac{L_S.\frac{S_S}{S_m}.K_S+K_m+L_p.\frac{S_p}{S_m}}{L_S.\frac{S_S}{S_m}+1+L_p.\frac{S_p}{S_m}} \quad (7)$$

Final resistance value is computed from multiplying initial static resistance and the conservative coefficient K_t as shown in equation 8:

$$R_{\text{final}} = K_tR_{\text{initial}} \quad (8)$$

This will allow the computation of the final static resistance for all three piles of row E in terms of time.

RESULTS

For a first setup process analysis, several series of driving and re-driving tests were carried out on the test piles. The piles' embedded length and their driving resistance (in terms of total number of hammer blows per 10-centimeter drive) are shown in Table-3.

ARPN Journal of Engineering and Applied Sciences

Table-3. Number of blows per 10-centimeter drive for each driving and re-driving set.

Pile	Phase	Set	Number of blows	Embed (cm)	Energy (KJ)	Blows per 10 cm at 250KJ
Pile EE90	Driving	Last set	25	10	255	26
	Re-driving	First set	10	2	220	44
		Third set	40	9.5	239	40
		Fourth set	40	6.7	237	57
Pile EC90	Driving	Last set	11	10	224	10
	Re-driving	First set	10	7.5	224	12
		Second set	40	33	236	11
Pile EA90	Driving	Last set	14	10	220	12
	Re-driving	First set	10	5	229	18
		Second set	40	32	241	12
		Third set	20	18	237	11
Pile EC91	Driving	Last set	15	10	213	13
	Re-driving	First set	10	6	213	14
Pile EA92	Driving	Last set	20	10	250	20
	Re-driving	First set	28	10	251	28
		Second set	26	10	256	27
		Third set	25	10	251	25
		Fourth set	29	10	251	29
		Fifth set	26	10	253	26
		Sixth set	27	10	251	27
		Seventh set	40	15	250	27
		Eighth set	40	15	253	27
Pile EE95	Driving	Last set	10	7	256	15
	Re-driving	First set	40	16	255	26
Pile EE92	Driving	Last set	16	10	240	15
	Re-driving	First set	32	17	270	20
Pile EA95	Driving	Last set	10	4	243	24
	Re-driving	First set	40	12	253	34
		Second set	40	17	253	24
		Third set	40	19	262	22
		Fourth set	40	20	258	21

According to the data shown in Table-3, setup appears as an increase in the number of blows necessary to drive the pile every 10 centimeters during the first driving sets, compared to that of the end of driving phase (FB). The setup process observed in the other series of driving is canceled because the soil is disturbed, once again.

The number of blows required to drive the EE90 10cm pile increased from 24 at the end of driving to 44 at the time of redriving after a period of 20 days. This significant increase in driving resistance is mainly caused by the soil setup phenomenon. Figure-4 shows an example of the driving resistance curve (number of blows for a 10-centimeter drive) against depth for the EE90 pile.

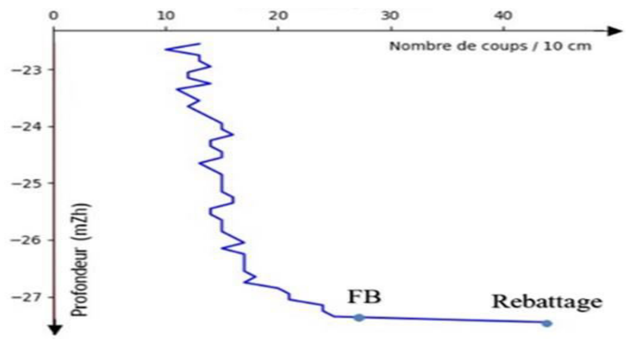

Figure-4. Driving resistance for pile EE90.

Results for global setup analysis for each of the piles and for different waiting times are shown in Table-4.

ARPN Journal of Engineering and Applied Sciences

Table-4. Setup analysis results for the studied piles at different waiting periods.

Pile	Phase	Waiting period t (days)	Depth (meters)	Static resistance (CAPWAP)	Setup rate	R_t/R_{FB}*
EA90	End-of-driving (FB)	-	-	7.03	69%	1.69
	Re-driving (RB)	17	-34.7	11.91		
EA92	FB	-	-	8.51	58%	1.58
	RB	13	-35.7	13.41		
EA 95	FB	-	-	9.1	34%	1.34
	RB	9	-36.04	12.18		
EE92	FB	-	-	10.03	40%	1.4
	RB	20	-34.99	14.01		
EE95	FB	-	-	10.13	30%	1.3
	RB	11	-34.78	13.16		
EE90	FB	-	-	9	47%	1.47
	RB	7	-35.06	13.26		
EC91	FB	-	-	7.62	9%	1.09
	RB	5	-34.68	8.33		
EC90	FB	-	-	6.55	25%	1.25
	RB	6	-34.65	8.21		

* R_t is the driving resistance at re-driving start after a waiting period of t days; R_{FB} is the end-of-driving resistance

Following the aforementioned results, all piles studied showed an increase in resistance to re-driving. However, we noted that the EC91 pile recorded the lowest setup ratio. The test at the end of the driving measured a resistance of 7.62 MN and re-driving showed a small increase of 9% for a total 8.33 MN. Since the re-driving test was carried out 5 days after the end of the beating, this waiting period is seen as insufficient for the setup process to complete.

Applying the Skov & Denver model to the measured resistances (Table-4) made it possible to determine the A parameter of the eight piles that were studied. Obtained results fall within the [0.13-0.56] interval, which is in agreement with the results of both Chow (1998) and Murad (2014). We will use an average value for A, which is 0.38. As for the Svinkin and Skov model, the average value of its parameter "B" is 0.19.

Figure-5 plots the predicted curves by the Skov & Denver (A = 0.38) and the Svinkin & Skov (B = 0.19) models in comparison with the obtained results. The correlation coefficients are respectively 0.77 and 0.75 for both models, which are seen as unsatisfactory. Thus, the two models do not accurately reflect resistance evolution in the study area and other influencing factors must be taken into account.

VOL. 18, NO. 22, NOVEMBER 2023 ISSN 1819-6608
ARPN Journal of Engineering and Applied Sciences

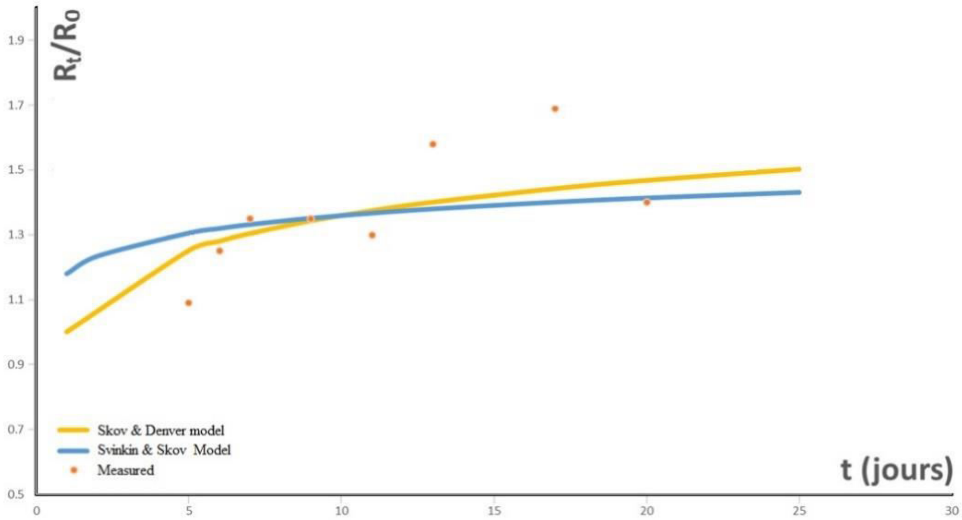

Figure-5. Evolution of setup for both Skov & Denver and Svinkin models compared to the study's setup rates.

At this stage, a more in-depth study was carried out by analyzing tip resistance and lateral friction contributions in the improvement of total resistance after driving phase as represented in Table-5.

Table-5. Friction and tip resistance increase computed with the CAPWAP software.

Pile	Phase	Resistance			Setup rate			Rt/R_0		
		Total	Friction	Tip	Total	Friction	Tip	Total	Friction	Tip
EA90	End-of-driving	7.03	5.49	1.54	69%	88%	4%	1.69	1.88	1.04
	Re-driving	11.91	10.31	1.6						
EA92	End-of-driving	8.51	6.24	2.27	58%	77%	4%	1.58	1.77	1.04
	Re-driving	13.41	11.04	2.37						
EA 95	End-of-driving	9.1	4.2	4.9	34%	65%	7%	1.34	1.65	1.07
	Re-driving	12.18	6.92	5.26						
EE92	End-of-driving	10.03	7.31	2.72	40%	51%	10%	1.40	1.51	1.10
	Re-driving	14.01	11.03	2.99						
EE95	End-of-driving	10.13	5.18	4.95	30%	42%	17%	1.30	1.42	1.17
	Re-driving	13.16	7.36	5.8						
EE90	End-of-driving	9	7.08	2.72	35%	46%	8%	1.35	1.46	1.08
	Re-driving	13.26	10.32	2.94						
EC91	End-of-driving	7.62	5.68	1.94	9%	11%	3%	1.09	1.11	1.03
	Re-driving	8.33	6.33	2						
EC90	End-of-driving	6.55	5.54	1.01	25%	28%	9%	1.25	1.28	1.09
	Re-driving	8.21	7.11	1.1						

Table-5 shows that both friction and tip resistances increase with time after the driving phase. However, the increase in resistance by friction varies from 11% to 88%, while that of the tip is limited to between 3% and 17%. This confirms that the setup phenomenon is mainly due to increased friction (Chow, 1998).

Thus, we will focus in what follows on the analysis of setup by friction, by taking into consideration soil layers crossed separately: a layer-by-layer analysis. For this, dynamic loading tests and a CAPWAP analysis gave the static friction resistances for each of the soil layers surrounding the pile. The ratios R_f/R_0 and setup rates $\Delta R/R_0$ are shown in Table-6.

ARPN Journal of Engineering and Applied Sciences

Table-6. Friction resistance evolution for sand and marl.

Pile	Waiting period (days)	Sand				Marl			
		R_0	R_f	$\Delta R/R_0$	R_f/R_0	R_0	R_f	$\Delta R/R_0$	R_f/R_0
EA90	17	0.392	0.519	32%	1.324	5.098	9.791	92%	1.921
EE 92	20	1.583	2.182	38%	1.378	3.961	8.845	123%	2.233
EC90	6	1.583	1.872	18%	1.183	3.961	5.298	34%	1.338
EC91	5	0.961	1.091	14%	1.135	4.719	5.239	11%	1.110
EE90	7	1.785	2.249	26%	1.260	5.291	7.821	48%	1.478
EA92	13	0.305	0.391	28%	1.282	5.933	10.649	79%	1.795
EE95	11	1.282	1.622	27%	1.265	3.598	6.325	76%	1.758
EA95	9	1.365	1.719	26%	1.259	5.945	9.311	57%	1.566

The main observation was that almost all soil layers showed significant setup. Maximum recorded evolution was for pile EE92, where a 20-day waiting period before re-driving shows a significant increase in the friction resistance of the layer of sand (38%) and of the marl (123 %).

As for the EC91 pile, it shows the least significant setup with an increase in friction with sand of 14% and with marl of 11%. This is due to the very short delay between the end-of-driving phase and the re-driving phase (5 days). Moreover, and unlike the other piles, the setup rate of the EC91 pile is higher in the sand layer than in the marl layer. This disparity is explained by the sand's permeability, which allows a faster dissipation of the overpressure compared to marl. Thus, the marl layer requires more than 5 days achieving significant setup rates.

The disparity between sand and marl results leads us to develop a new approach that treats both soil types separately. It starts with a layer-by-layer analysis of the setup process with the Skov and Denver model as shown in Figure-6. Setup parameter "A" calculation is based on an initial reference time t_0 of 12 hours for sand and one day for marl.

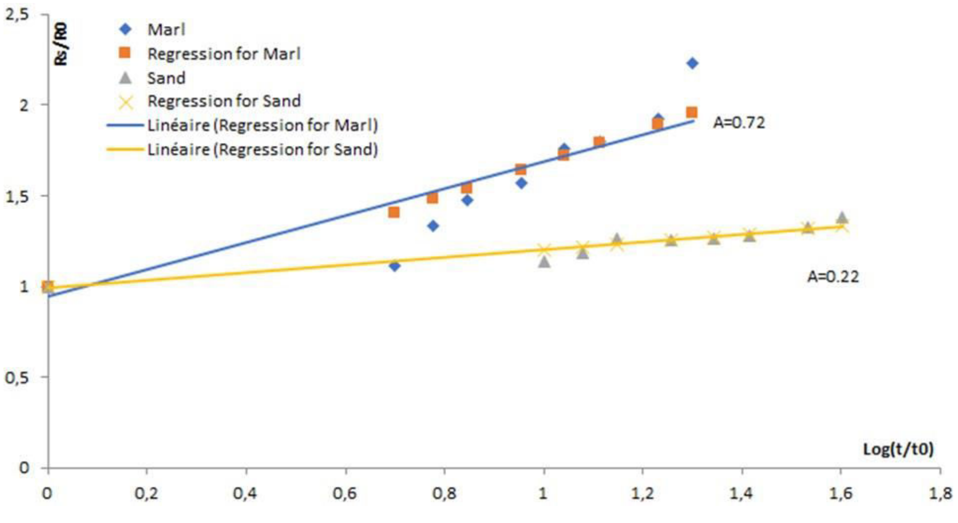

Figure-6. Linear regression against resistance ratio with logarithmic time in sand and marl

Setup evolution against time for both sand and marl using the Skov and Denver model is shown in Figure-7.

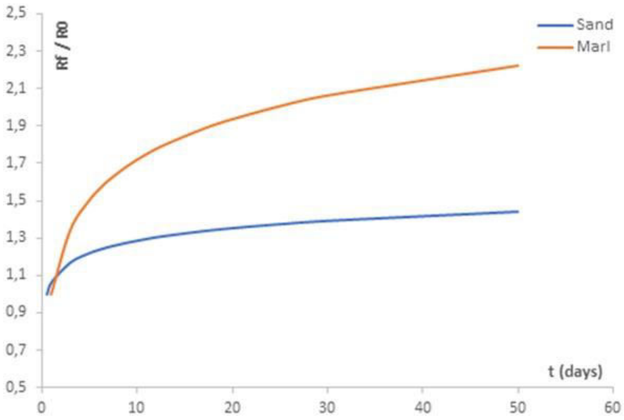

Figure-7. Setup evolution with the Skov and Denver model for sand (A=0.22) and marl (A=0.72).

As stated previously, Figure 6 clearly shows that setup in the marl layer is greater than in the sand layer. Moreover, the linear regression of the R_f/R_{FB} setup ratio with logarithmic time fits the obtained results very well (R^2=0.94 and R^2=0.97 for sand and marl respectively), which confirms the suitability of the Skov and Denver model for the tested piles. The obtained parameter A is 0.22 for sand and 0.72 for marl. These values are consistent with results found in Louisiana, USA sites (Murad, 2014). However, this model has a limitation relating to a non-zero benchmark time estimation, hence the idea of developing a new power equation form which would take into account an immediate setup effect (which is activated right after the end-of-driving and before the initial benchmark time t_0). A general formula of the new model is expressed as follows:

$$\frac{R_f}{R_{FB}} = at^b \tag{9}$$

Where:

- **t:** elapsed time after end-of-driving phase
- $\mathbf{R_f}$**:** Friction resistance at given time t
- $\mathbf{R_{FB}}$**:** Resistance at end-of-driving
- **a and b:** empirical coefficients

The model based on the power function has been proposed with different a and b coefficients (Svinkin, 1996; Long *et al.*, 1999; Lutful and Decapite, 2011) depending on soil data and conditions as well as loading test results. In this analysis, and using Python programming, two models were developed (for sand and marl) as follows:

- For sand:

$$\frac{R_f}{R_{FB}} = 0.96\ t^{0.114} \tag{10}$$

- For marl:

$$\frac{R_f}{R_{FB}} = 0.62\ t^{0.42} \tag{11}$$

Correlation coefficients' values for both proposed models are satisfactory (0.944 for sand and 0.980 for marl) and even exceed those of the Skov and Denver model. This means that the proposed model provides a better fit for our data and grants both higher accuracy and reliability in predicting post-driving soil setup.

A comparison of measured resistances against estimated resistances is presented in Figure-8.

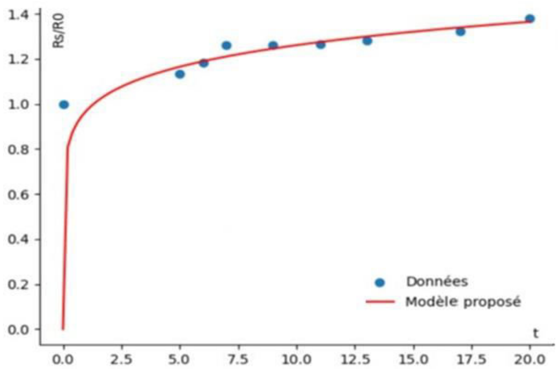

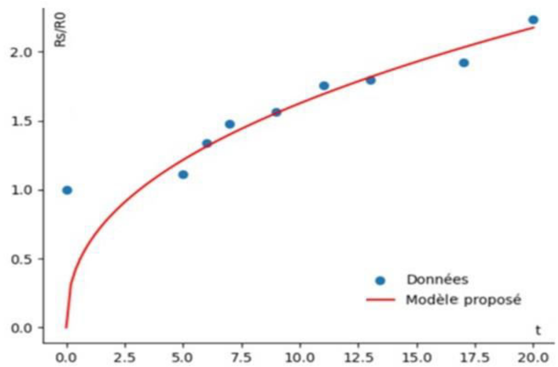

Figure-8. Results for the proposed model based on the power function for sand (on the left) end for marl (on the right).

At this stage, where the setup model is satisfactory, the piles' final static resistance can be computed according to equation 8, which clearly shows a progressive increase in resistance over time. This observation is beneficial in the event of non-compliance with the driving refusal criteria; meaning if the design's static resistance has not been achieved. In this case, we can affirm that resistances will comply after a certain number of days.

The final static resistance is calculated by considering values obtained by the suggested power function model for the following sand and marl setup rates K_S and K_M:

- For sand:

$$KS = \frac{R_f}{R_{FB}} = 0.96\ t^{0.114}$$

- For marl:

$$KM = \frac{R_f}{R_{FB}} = 0.62\ t^{0.42}$$

 ISSN 1819-6608
ARPN Journal of Engineering and Applied Sciences

Table-7 shows the increase in the conservative coefficient K_t (equation 7) and the static resistance of piles EE90, EE92 and EE95 against time. This approach can also be applied to other rows of piles.

Table-7. Final resistance of piles after soil setup for different waiting periods.

Number of days j		**5**	**10**	**15**	**20**	**25**	**30**
K_J		1.153	1.378	1.540	1.671	1.784	1.884
R_{final}	pile EE90	10.375	12.403	13.862	15.046	16.059	16.955
	pile EE92	11.562	13.822	15.449	16.767	17.897	18.895
	pile EE95	11.678	13.960	15.603	16.935	18.075	19.084

Considering the proposed power function model, if the design's static resistance is valued at 15 MPa for the EE90, EE92 and EE95 piles at end-of-driving phase, and if the obtained static resistance on site is less than 15 MPa, we can safely predict that this number will be reached after 15 days at most for the EE92 and EE95 piles and after 20 days at most for the EE90 pile.

INTERPRETATIONS

A. Why setup is mainly due to increased friction? Indeed; there is a difference in the stress transfer mechanisms between the pile's shaft and tip:

a) Frictional resistance is based on the interaction between the pile shaft and surrounding soil over a considerable length. When the pile is driven into the ground, the latter moves (displaces), compacts, consolidates and settles over time thus forming a stronger interface between the pile and the ground which facilitates stress transfers, leading to an increase in frictional resistance. On the other hand, tip resistance mainly depends on the interaction between the pile's tip and the lower soil, which limits the setup effect to a more restricted area around the tip.

b) Over time, setup continues by constantly strengthening the soil-pile interface, leading to a gradual increase in frictional resistance. This cumulative process grants frictional resistance a more important contribution to soil setup while continuously influencing the pile's bearing capacity significantly. On the other hand, tip resistance may be more influenced by initial conditions or immediate interactions during driving.

B. It was observed that the setup potential is greater in the marl layer than in the sand layer. This could be interpreted as follows:

a) Marls are cohesive soils due to their clayey composition. Thus, they're able to reorganize and re-stabilize after pile driving, unlike sands which are less cohesive.

b) When the pile is driven into the marl, it tends to compact more around the pile, offering better stability, unlike sands which tend to loosen.

c) Marl, being a clayey soil, has a greater water retention capacity compared to sand. By retaining water, marl facilitates pore pressure redistribution and allows for a slower and more regular dissipation, which contributes to more effective setup. On the other hand, and due to their granular structure (higher porosity), sands have a lower water retention capacity allowing water to flow more easily. Therefore, sand does not effectively dissipate pore pressure, which can negatively impact setup.

CONCLUSIONS

When the soil crossed by the pile is multi-layered, its behavior changes from one layer to another during driving. Indeed, the interactions of the soil layers with the pile and their impacts on the setup process are as different as their characteristics and properties vary.

The adopted approach in this study makes it possible to confidently estimate the maximum waiting time to reach the required bearing capacity. Thus, it encourages relying on the gradual natural setup of the soil instead of rushing to take immediate and costly measures such as patching works.

It should be noted that this approach is based on conservative estimates which ensure an adequate safety margin in attained resistances against design requirements. It makes it possible to manage resources, costs and construction times more efficiently, while maintaining appropriate levels of safety.

REFERENCES

Bullock P. J. 1999. Pile friction freeze: A field and laboratory study, Ph. D Dissertation, University of Florida.

Bullock P. J., Schmertmann J. H., McVay M. C. and Town- send F. C. 2005a. Side Shear Setup. I: Test Piles Driv-en in Florida. J. Geotech. Geoenviron. Eng. 131(3): 292-300.

Chow F. C., Jardine R. J. and Nauroy J. F. 1998. Effects of Time on Capacity of Pipe Piles in Dense Marine Sand. J. Geotech. Geoenviron. Eng. 124(3): 254-264.

Camp III, W. M. and Parmar, H. S. 1999. Characterization of pile capacity with time in the cooper marl: A study of the applicability of a past approach to predict long term pile capacity, Transportation Research Record. 1663, 16-24.

Hosseini Mohammad amin. 2015. A thesis, Evolution of Pile Shaft Capacity over Time in Soft Clays (Case Study: Leda Clay).

Kam W. Ng, A.M. ASCE, Pile Setup in Cohesive Soil. I: Experimental Investigation. Journal of Geotechnical and Geoenvironmental Engineering.

Komurka Van E, A REVIEW OF PILE SET-UP, Department of Civil and Environmental Engineering. University of Wisconsin-Madison, Madison.

Komurka V. E., Wagner A. B. and Edil T. 200. Estimating soil/pile setup. Wisconsin highway research program #0092-00-14, Final Report.

Lysebjerg J. 2004. The Influence of Time on Bearing Capacity of Driven Piles. Proceedings of the 14th Nordic Geotechnical Meeting.

Long J. H., Kerrigan J. A. and Wysockey M. H. 1999. Measured time eŠects for axial capacity of driven piling, Transportation Research Record. 1663, 8-15.

Lutful K. and Decapite K. 2011. Prediction of Pile Setup for Ohio Soils. Report No. FHWA/OH-2011/3, Ohio Department of Transportation, Cleveland, OH.

Murad Abu-Farsakh. 2014. Field Investigation of Pile Setup in Mixed Soil. Article in Geotechnical Testing Journal.

Murad Y. Abu-Farsakh and Zhongjie Zhang. 2017. Evaluation of pile capacity from CPT and pile setup phenomenon. Inter-national Journal of Geotechnical Engineering.

Murad Y. Abu-Farsakh. 2018. Development of analytical models to estimate the increase in pile capacity with time (pile setup) from soil properties.

Paikowsky S. G. and Hajduk E. L. 2005. Comparison between Model and Full Scale Pile Capacity Gain in Boston Area. Proc., Advances in Deep Foundations: Geo-Frontiers Congress, Austin, Tex.

Rami Ksaibati. 2018. Effect of Soil Layering on Shorter-Term Pile Setup. American Society of Civil Engineers.

Schmertmann J. H. 1991. The Mechanical Aging of Soils, 25th Terzaghi Lecture. Journal of Geotechnical Engineering, ASCE. 117(9): 1288-1330.

Skov R. and Denver H. 1988. Time-Dependence of Bearing Capacity of Piles. Proc., 3rd International Conference on the Application of Stress-Wave Theory to Piles, Vancouver, British Columbia, Canada. pp. 879-888.

Skov R. and Svinkin M. R. 2000. Setup Effect of Cohesive Soils in Pile Capacity. Proceedings of the 6th International Conference on Application of Stress Waves to Piles, Sa˜o Paulo, Brazil. pp. 107-111.

Svinkin M. R., Morgano C. M. and Morvant M. 1994. Pile capacity as a function of time in clayey and sandy soils. Deep Foundations Institute 5th International Conference and Exhibition on Piling and Deep Foundations, Belgium.

Svinkin M. R. 1996. Setup and relaxation in glacial sand-discussion. Journal of Geotechnical Engineering, ASCE. 122(4): 319-321.

Svinkin M. R. and Skov R. 2000. Setup effects of cohesive soils in pile capacity, Proc. 6th International Confer-ence on Application of Stress-Wave Theory to Piles, Sao Paulo, Brazil, Balkema. 107-111.

Svinkin M. R., Morgano C. M. and Morvant M. 1994. Pile Capacity as a Function of Time in Clayey and Sandy Soils. In Proceedings of the 5th DFI International Conference, Rome, Italy. pp. 451-456.